

Principles and properties of phononic crystal waveguides

Cite as: APL Mater. 9, 080701 (2021); <https://doi.org/10.1063/5.0059035>

Submitted: 04 June 2021 . Accepted: 29 July 2021 . Published Online: 13 August 2021

 V. Laude

COLLECTIONS

Paper published as part of the special topic on [Phononic Crystals at Various Frequencies](#)



View Online



Export Citation



CrossMark



[silicon nanowires](#) [glucose carbon](#) [fluoropolymers](#) [fused silica](#) [additive manufacturing](#)
[sulfides](#) [III-V semiconductors](#) [gallium nitride](#) [copper nanoparticles](#) [organometallics](#)
[nano ribbons](#) [barium fluoride](#) [nanoporous polymers](#) [perovskites](#) [infrared dyes](#)
[epitaxial crystal growths](#) [ultra high purity materials](#) [transparent oxides](#) [CIGS](#)
[cerium oxide polishing powder](#) [surface functionalized nanoparticles](#) [carbon nanotubes](#) [nanodispersions](#)
[MOCVD](#) [beta barium borate](#) [DLED lighting](#) [solar energy](#)
[rare earth metals](#) [quantum dots](#) [cutting blades](#) [fiber optics](#)
[cerium](#) [sulfuric acid](#) [Inkjet](#) [deposition slugs](#) [CVD precursors](#) [photovoltaics](#)
[structural metals](#) [kapor crystals](#) [meta materials](#) [aerogels](#) [glass](#)
[anode](#) [lithium nitrate](#) [HAs wafers](#) [superconductors](#) [indium tin oxide](#) [WGa2](#) [nanos](#)
[exposures](#) [selfies](#) [MOs](#) [Au/Ni](#) [diamond microsawdust](#) [optical glass](#)
[chalcopyrites](#) [ZnS](#) [CoTe](#) [perovskite crystals](#) [transparent ceramics](#)

The Next Generation of Material Science Catalogs

www.americanelements.com




Principles and properties of phononic crystal waveguides

Cite as: APL Mater. 9, 080701 (2021); doi: 10.1063/5.0059035

Submitted: 4 June 2021 • Accepted: 29 July 2021 •

Published Online: 13 August 2021



View Online



Export Citation



CrossMark

V. Laude^{a)} 

AFFILIATIONS

Institut FEMTO-ST, CNRS UMR 6174, Université Bourgogne Franche-Comté, 25030 Besançon, France

Note: This paper is part of the Special Topic on Phononic Crystals at Various Frequencies.

^{a)} Author to whom correspondence should be addressed: vincent.laude@ubfc.fr

ABSTRACT

Strongly confined waveguiding is one of the main applications of phononic crystals that can be achieved at any frequency and scale. Phononic crystal waveguides replace the cladding of classical homogeneous waveguides by a crystal possessing a complete phononic bandgap. We review the different material systems used to implement phononic crystal waveguides and how waveguiding is obtained by confining waves in a core or by coupling defects along a given direction. Finally, we introduce topological principles to design defect-less waveguides by exploiting the symmetry of crystals.

© 2021 Author(s). All article content, except where otherwise noted, is licensed under a Creative Commons Attribution (CC BY) license (<http://creativecommons.org/licenses/by/4.0/>). <https://doi.org/10.1063/5.0059035>

I. INTRODUCTION

The ability to conceive waveguiding devices by relying upon the physical properties of phononic crystals has, from the beginning, been a major incentive toward the development of this field at the crossroad of condensed matter physics, physical acoustics, wave physics, and engineering.¹⁻³ A phononic crystal is an artificial and periodic structure that supports the propagation of mechanical waves. By artificial, we refer to its technological fabrication process, by a human or a machine, at almost any available scale. The specification of periodicity is also very important and is the source of the existence of frequency bandgaps, inside which no propagating waves are allowed, only evanescent waves. Actually, the very term “phononic” before crystal means that it has a band structure similar to the band structure of phonons in crystal lattices. In Sec. II, we discuss the main material systems that have been considered in the literature for the fabrication of phononic crystals and briefly summarize why they have been.

Guiding waves is an important problem for both science and technology. Nowadays, optical fibers supporting the propagation of light waves are ubiquitous for building communication networks and the internet. Acoustic musical instruments include guides for sound waves. Elastic waves guided by rails and pipes are used to monitor their structural health. The physical mechanism for guidance can be based on boundary conditions only or on the

spatial distribution of the material constants in the structure. Only the latter option is relevant to our discussion. In a classical homogeneous waveguide the structure is invariant in a given direction, as depicted in Fig. 1(a). Waves are guided in a core surrounded by a cladding. In the dispersion diagram represented in Fig. 1(b), giving the reduced frequency ωd as a function of the reduced wavenumber kd , with d being the diameter of the core, the dispersion relation for guided waves must appear in the cone delimited by two wave lines. The slope of the bottom line is given by the wave velocity in the core, whereas the slope of the top line is given by the wave velocity in the cladding, i.e., we have assumed the velocity of waves to be smaller in the core compared to the cladding. Apart from this condition, guided wave propagation can be monomodal or multimodal, depending mostly on the diameter of the core compared to the wavelength $\lambda = 2\pi/k$.

In a phononic crystal waveguide, the homogeneous cladding material is replaced by a heterogeneous phononic crystal, but the core can be kept unchanged or not. The situation is depicted in Fig. 1(c). For waves to be guided, there must be only evanescent waves in the cladding, and hence a complete phononic bandgap is compulsory. Obviously, the operation bandwidth of a phononic crystal waveguide cannot exceed the bandgap width. As a corollary, the larger the bandgap, the more the bandwidth is available. Since the phononic crystal waveguide is periodic along its principal axis, the dispersion diagram becomes a phononic band structure, as

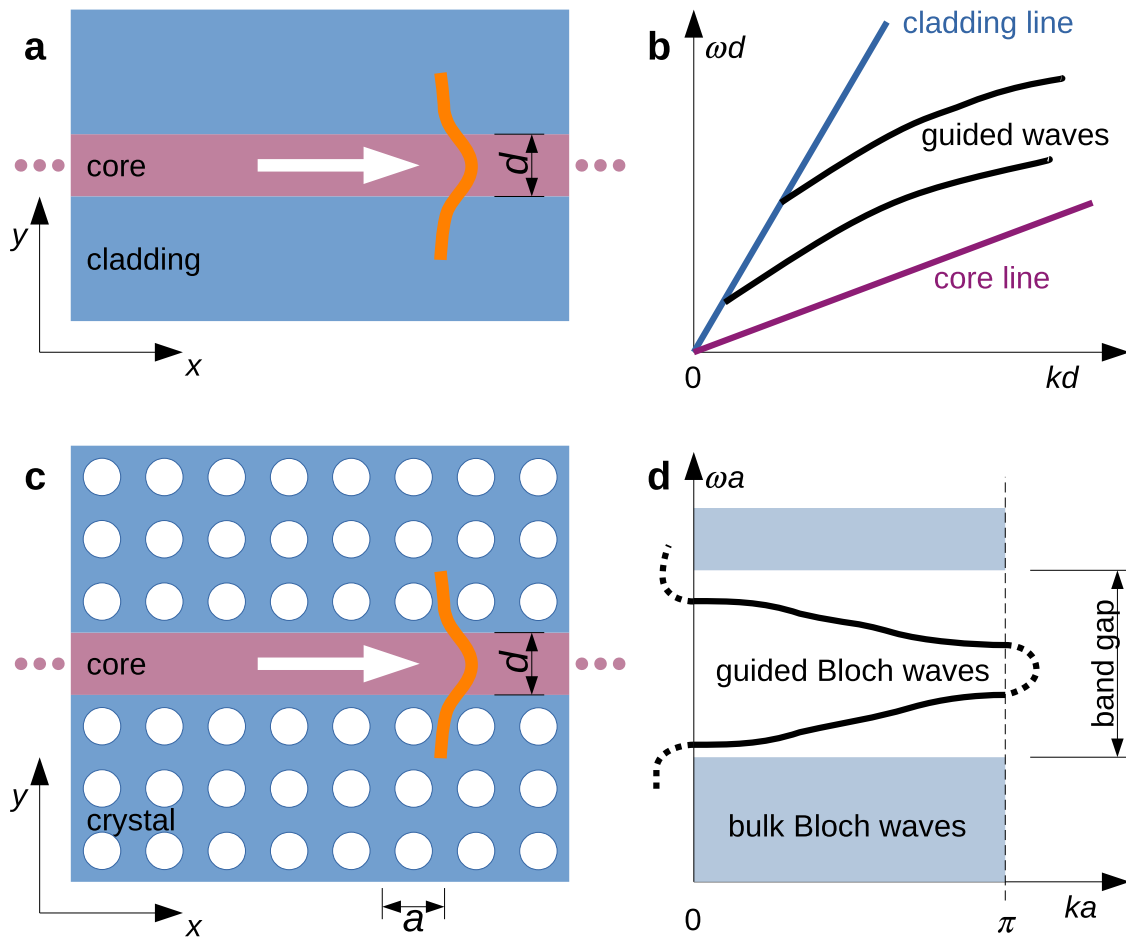


FIG. 1. Waveguide principles. (a) The homogeneous waveguide is a structure composed of a core and a cladding. If the velocity of waves is smaller in the core than in the cladding, then guided waves are laterally evanescent in the cladding, though propagating in the core. (b) The dispersion of guided waves in a homogeneous waveguide extends in the region delimited by two sound lines, one for the core and one for the cladding. (c) A phononic crystal with a complete bandgap replaces the cladding in phononic crystal waveguides. (d) As the phononic crystal waveguide is periodic along its principal axis, the dispersion of guided waves extends for frequencies inside the bandgap and for Bloch wavenumbers defined in the first Brillouin zone. Guided bands fold at zone boundaries and can enter guided bandgaps.

illustrated in Fig. 1(d). Periodicity implies that guided bands can fold at the edges of the first Brillouin zone, just as the bulk bands of the crystal do. As a result, bandgaps for guided waves can appear inside the bulk bandgap. Such foldings and bandgap openings result from the interference of guided waves propagating to the right with the guided waves propagating to the left. In case such interferences occur, a consequence is that the available waveguiding bandwidth cannot be completely used in practice.

As for any waveguiding structure, there are technologically important questions that must be answered to properly evaluate the interest of a particular design or structural choice. What is the degree of spatial confinement that is provided by the phononic crystal cladding, how does it relate to the available bandwidth, and should we expect propagation loss? Section II considers these questions in direct relation to the choice of the material system. What is the dispersion relation for guided waves and how can it be tuned to given purposes? The answer generally means engineering of the design of

the core; Sec. III considers linear waveguides built around a homogeneous core, whereas Sec. IV considers instead the coupling of defect cavities forming a guiding core. Can we guarantee monomodal operation, can we minimize backscattering loss, and do we really need a core for wave guidance? To answer these questions, Sec. V incorporates the novel vision brought by topological physics and its relations with symmetry.

II. MATERIAL SYSTEMS ACCESSIBLE TO EXPERIMENT

In this section, we review shortly the different material systems that have been considered for the realization of phononic crystal waveguides. In either case, we give the range of frequencies that is available and the potential losses and discuss possible limitations. Regardless of these specificities, the concepts discussed in Secs. III–V apply to all of them, making phononic crystal waveguides available over a wide frequency and scale range.

Airborne sound is well suited in the audible range (from a few Hertz to about 10 kHz) and up into the ultrasonic range. Since air is notably soft and light, especially compared to rigid walls enclosing an atmosphere, airborne acoustic waves hardly excite acoustic waves in water or elastic waves in usual solids (e.g., concrete, plastic, steel, or wood). Hence, sonic crystals for airborne sound are easily modeled as a single phase material enclosed by hard boundaries. They have downsides, though, since they suffer thermo-viscous loss and low frequencies mean long wavelengths and hence long lattice constants. For the latter reason, they are often considered in a waveguide configuration for confinement in the third direction,⁴ as depicted in Fig. 2(a), based on the fact that air slabs do not have a frequency cut-off. For the thickness of the slab $h \ll \lambda$, the sonic crystal slab can be effectively modeled as a 2D crystal.

The case of solid inclusions in a fluid has often been considered in conjunction with ultrasonic transducers operating for frequencies between 100 kHz and a few MHz, especially with a lattice of steel rods immersed in water. This type of sonic crystal, depicted in Fig. 2(b), approximates a 2D system that is infinite in the third direction. Viscous loss in water is limited, permitting operation at high ultrasonic frequencies. The case of a heavy and stiff solid material is favorable for large phononic bandgaps. On the modeling side,

coupling of acoustic waves in the fluid and elastic waves in the solid must be taken into account for accurate numerical results.³

The case of holey crystals depicted in Fig. 2(c) is technologically very important. Lattices of holes in a solid plate or slab appear frequently with microelectromechanical system (MEMS) structures at ultrasonic frequencies and micron sizes⁵⁻⁷ and at the smaller scale with optomechanical structures operating at a few GHz (lattice constants of a few 100 nm).⁸⁻¹⁰ Viscoelastic losses can be rather limited, especially with single-crystal materials, such as silicon, quartz, or sapphire. In case there is a supporting substrate underneath the finite-thickness holey crystal, phononic crystals for surface acoustic waves (SAWs) can be fabricated. In this case, a piezoelectric substrate or layer is frequently considered, including lithium niobate or zinc oxide. As a note, a circular hole is usually not the best choice for the shape of the inclusion if one wants to maximize the phononic bandgap width; square-lattice crystals of cross holes¹¹ or hexagonal-lattice crystals of snowflake holes⁸⁻¹⁰ are successful solutions, and more complex unit-cells can be conceived through topology optimization or rational design.

As an alternative to crystals of holes, one can consider solid inclusions embedded in a plate,¹²⁻¹⁵ as depicted in Fig. 2(c). Millimeter size beads can be included in an epoxy matrix, for instance,

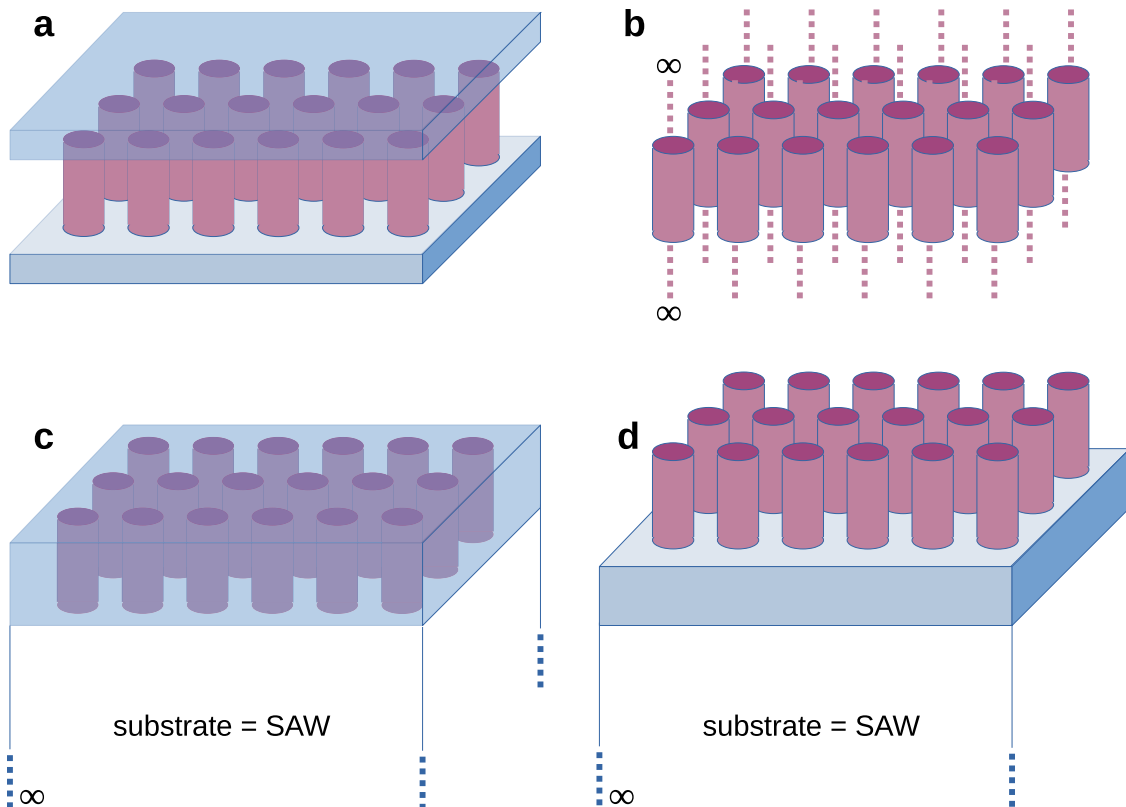


FIG. 2. Schematic of two-dimensional crystal structures amenable to experiments. (a) A 2D periodic array of rods sandwiched between two parallel plates forms a waveguide for sound waves in air. (b) The same array of rods, if they can be considered infinitely long, forms a 2D phononic crystal; such an arrangement is often used for acoustic waves in water. (c) Cylindrical holes or solid rods in a plate form a phononic crystal slab for elastic waves; if the slab is supported by a semi-infinite substrate, surface acoustic waves (SAWs) must be considered. (d) Cylindrical rods or pillars sitting on a plate can be considered alternatively; again, they can be combined with a supporting semi-infinite substrate.

or wafer-level technologies can be used at the microscale. Growing pillars on a surface is often technologically less demanding^{16,17} [see Fig. 2(d)]. Inclusions and pillars provide one with additional degrees of freedom, as they can act as local resonators storing mechanical energy and interacting with the waves propagating in the substrate. The so-called locally resonant crystals have been used as a basis to create crystal waveguides for Lamb waves in plates^{18–20} and SAW on substrates.^{21,22}

III. LINEAR DEFECT WAVEGUIDES

The first designs of phononic crystal waveguides were naturally based on the idea of replacing the cladding by a complete bandgap crystal while keeping a homogeneous core.^{23–25} Straight and bent waveguides and more general circuits are readily imagined, as depicted in Fig. 3(a). Naively, it may be thought that because waves are evanescent in the cladding but propagating in the core,

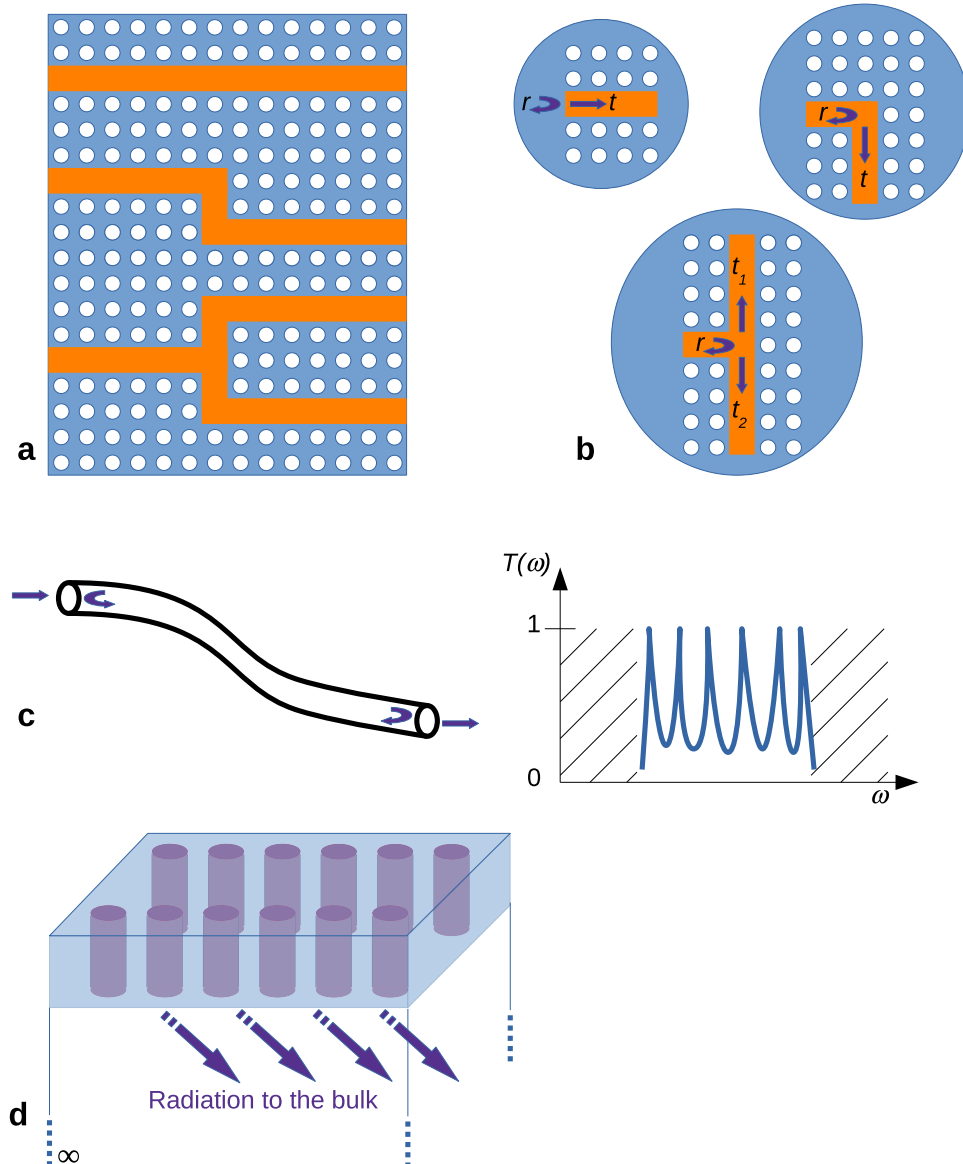


FIG. 3. Schematic of the concepts of linear defect waveguides. (a) Different linear, bent, and multiplexed structures can be imagined. (b) Whenever periodicity is locally broken, guided waves are reflected and transmitted to the available normal modes. (c) Because there is a strong impedance and structural mismatch at the entrance and the exit of a phononic crystal waveguide, a channeled spectrum can generally be expected in the transmission through the waveguide. (d) Specifically, in the case of a supporting semi-infinite substrate, radiation to the bulk modes can occur.

their dispersion will be similar to that of bulk waves in the homogeneous core material. This idea definitely proves incorrect. Actually, when a defect is introduced inside an otherwise perfectly periodic crystal, modes localized around the defect must appear. If a whole row of defects is introduced to create a core, then waveguiding bands appear as the result of the axial coupling of the sequence of defects. From a theoretical point of view, the number of periodicities of the crystal is reduced by one and the band structure for guided waves can be computed with a supercell technique. This model leads to a re-interpretation: the defective supercells are very strongly coupled axially, thus leading to highly dispersive and interfering bands.^{26–29} Furthermore, bandgaps for guided waves can appear at the

symmetry points of the Brillouin zone of the super-cell, as we explained in the Introduction. Another consequence is that guided bands tend to become flat and the group velocity is noticeably reduced compared to the homogeneous core.³⁰

Once a guided mode is excited inside a straight core, it will propagate with little perturbations because the eigenmodes of a crystal are translationally invariant. Misalignments and errors of fabrication lead to moderate scattering and energy transfer between the normal guided modes. Difficulties arise, however, whenever periodicity is broken,³¹ as depicted in Fig. 3(b). First, it is difficult to couple from the exterior to the inside of the core because of the generally strong modal mismatch between the two rather

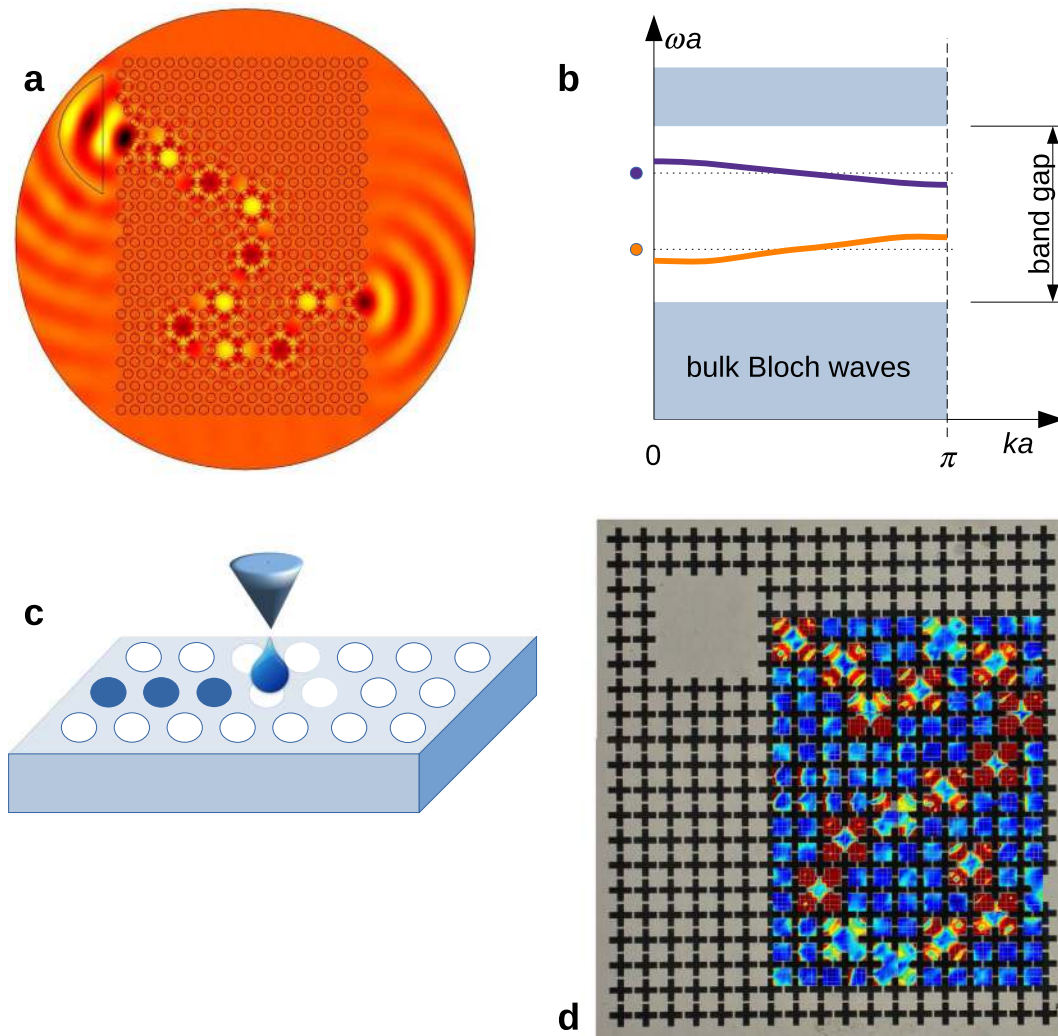


FIG. 4. Schematic of the coupled-resonator acoustic waveguide (CRAW) concept. (a) Defects spaced by a few lattice constants form a CRAW in a hexagonal-lattice crystal. (b) The dispersion relation inside the complete phononic bandgap is composed of very flat periodic bands centered around the resonance frequencies of the defect. (c) Reconfigurable and reusable phononic circuits can be implemented by selective filling of hollow cavities in a solid phononic crystal. (d) Experimental measurement of surface vibrations confirms that guided waves in a CRAW have no obligation to take straight lines (experimental data obtained with the sample of Ref. 44). The square-lattice array of cross holes has a lattice constant of $715 \mu\text{m}$, the plate thickness is $500 \mu\text{m}$, and the operation frequency is $\approx 2.5 \text{ MHz}$.

different regions of space. A similar observation holds by reciprocity: at the end of the waveguide, large reflection/small transmission can occur for the guided waves. Bends between straight waveguide sections can also induce significant reflections. From a practical point of view, phononic circuits can be modeled using scattering matrices accounting for reflection and transmission between normal modes. Elementary reflection and transmission coefficients are functions of frequency (are dispersive). For instance, even for a simple straight waveguide, the reflections occurring at the entrance and the exit lead to the formation of a channeled spectrum in the overall transmission function³² [see Fig. 3(c)].

Another issue specific to SAW is that surface guided waves are not perfectly confined in the third dimension and hence can radiate toward the bulk of the supporting substrate.^{33–35} That radiation is highly dispersive and is induced by the surface structuration, as depicted in Fig. 3(d). In the SAW case, normal mode theory does not apply anymore and one needs to consider quasi-normal, radiating, modes instead.³⁶ The sound line concept comes into the picture and allows us to isolate a certain region of dispersion space where radiation is canceled.³⁵

IV. COUPLED-RESONATOR ACOUSTIC WAVEGUIDES

Instead of considering directly adjacent defects forming a whole row and thus an homogeneous core, they are spaced a few lattice constants away. This idea, inspired originally by a similar photonic crystal concept,^{37,38} is exemplified in Fig. 4(a). The adjacent defects are separated by a small section of the phononic crystal; since the considered frequencies lie within a complete bandgap, they are coupled evanescently in their near-field. As a result, the strength of near-neighbor coupling decreases very fast with the separation of defects. Guided bands extend around the resonant frequencies of the defect surrounded by an infinite crystal. Their dispersion is directly dictated by the coupling coefficients between nearest-neighbor defects.^{39,40} They thus become separated and have a very smooth dispersion; furthermore, they become very flat and, thus, the available bandwidth is greatly reduced although very low group velocities can be achieved.⁴¹ Those properties are illustrated in Fig. 4(b).

One limitation of the concept of the coupled-resonator acoustic waveguide (CRAW) is that the original modes must be non-degenerate; otherwise, the situation becomes more complicated, with possible interference between guided bands occupying the same frequency bandwidth. Reconfigurable CRAW can be formed from a solid holey crystal filled selectively with a fluid,^{42,43} as depicted in Fig. 4(c). Each fluid-filled hole becomes naturally a local defect introducing new acoustoelastic modes and guided bands when they couple. Following that strategy, reconfigurable and reusable waveguides are formed.

Rather arbitrary circuits can be defined using the concept of CRAW, including multiple changes in the direction of propagation. Indeed, evanescent coupling is, in principle, valid in every direction, within a complete bandgap. What determines if defect modes can couple is their relative symmetry. Figure 4(a) already illustrated how guided waves hop from defect to defect inside a hexagonal crystal. Figure 4(d) shows the example of a square-lattice solid glass plate where defects are distributed along the path a knight could follow on a chessboard.⁴⁴

V. TOPOLOGICAL WAVEGUIDES

All waveguides discussed so far were based on the introduction of coupled defect states in a crystal. Starting from 2015 approximately, different guiding principles based on the topological properties of the phononic band structure started to emerge.^{45,46} This topological revolution was inspired originally by topological insulators^{47,48} and follows a similar trend in photonics. In the theory of the quantum Hall effect, edge states emerge in a bandgap if the bands below the gap have non-zero Chern numbers, an integer labeling the topological order of each particular band. By the bulk-boundary principle, the number of edge states equals the sum of the Chern numbers of bands below the bandgap; hence, they exist without requiring the presence of a core but only of an edge or an interface. The first implementation of topological ideas in phononics required breaking time-reversal symmetry. This can be performed with classical waves by imposing the propagation medium to move at some speed, for instance. Beyond the first experimental implementations at low frequencies,^{49–51} experimental difficulties to move to higher frequencies are immense, notwithstanding the case of GHz elastic waves. For that reason, we discuss in the following an alternative approach for passive systems, which is based on symmetry properties of the bulk crystal and their transformation in a topological transition.

A. Valley Hall crystals

Let us consider in Fig. 5(a) the **p6m** space group of a hexagonal crystal in the Hermann–Mauguin notation. The reciprocal lattice also has a hexagonal symmetry, characterized by the C_6v point group in Schoenflies notation. The primitive unit-cell is a parallelogram. The hexagonal lattice has a sixfold rotation center at corners of the unit-cell and two threefold rotation centers. M points lie half-way between zone centers, while K points are actually threefold rotation centers in reciprocal space. There are also many reflection symmetry axes that we do not detail but that typically join nearest cell centers or run along cell boundaries. The valley Hall type crystal proceeds by breaking slightly the symmetry of the hexagonal lattice, not touching rotations but reducing reflection symmetries, as depicted in Fig. 5(b). The first step is to replace the circular inclusion by a triangular inclusion.^{4,52} With the orientation angle $\alpha = 0^\circ$, the space group is changed to **p31m**: reflection axes are reduced to the horizontal axis. This reflection axis mirroring the threefold rotation centers is untouched. When $\alpha \neq 0^\circ$, the space group changes to **p3**; the previous reflection axis is lost and chirality is introduced in the crystal, lifting the degeneracy at the K and K' points and opening the bandgap at those points, as shown in Fig. 5(c).

As an example, let us consider the hexagonal-lattice sonic crystal composed of rigid triangular inclusions in an air background.⁴ As the angle of the inclusions is continuously tuned, the bandgap that was closed for $\alpha = 0^\circ$ gradually opens at the K point, reaching its maximum width for $\alpha = \pm 30^\circ$. The rotation of the inclusion is periodic with period 60° . The dispersion is further isotropic around point K (or K'), which in the hexagonal lattice results only from symmetry. A domain wall can then be formed by piling two instances of the crystal with opposite rotations. The domain wall must also be oriented along that axis, and the crystal cells must respect the hexagonal tiling of the plane. The resulting composite crystal is depicted

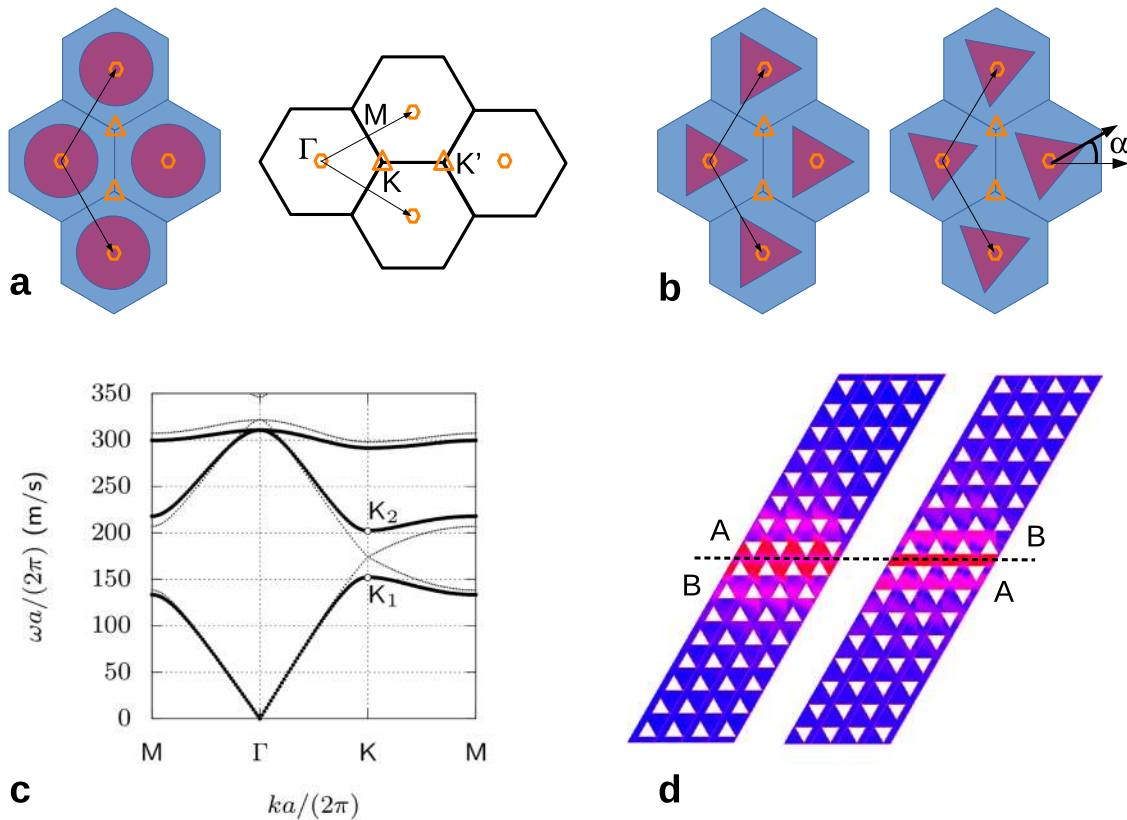


FIG. 5. Valley Hall crystals. (a) With highly symmetric inclusions, the hexagonal crystal is invariant under the $p6m$ space group and the reciprocal lattice is characterized by the C_6v point group. (b) Triangular inclusions reduce symmetry. (c) For non-rotated triangles, there is a Dirac cone forming at the K point of the Brillouin zone that breaks and opens a complete bandgap when triangles are rotated. The band structure is here shown for sound waves in air. (d) Two non-equivalent domain walls can be formed by piling two instances of the crystal with opposite rotations. Guided waves appear along the domain wall in the absence of defects.

in Fig. 5(d). Since there are two crystal phases, we can choose to place A over B or the converse. The band structures computed for super-cells AB and BA are identical. Two bands appear inside the bandgap: they are the dispersion of topological guided waves. The two bands cross without forming an avoided crossing, indicating that the corresponding Bloch waves are orthogonal.

Topological backscattering protection is a concept that is frequently put forward in comparison with defect crystal waveguides that do not possess that property. In the case of the valley Hall crystal, topological protection can be understood based on symmetry. There are indeed two orthogonal groups of bands, as a result of symmetry with respect to the axis of the waveguide. Robustness is dictated by the symmetry of the Bloch waves traveling to the right and to the left: the different bands of guided waves cross without interfering at the edges of the first Brillouin zone. As a result, within the crystal, they are protected from backscattering or modal conversion on scattering defects that preserve symmetry. There is no unidirectional propagation: the edge modes propagate both right and left, and the band structure is symmetrical in the exchange $k \leftrightarrow -k$. Any obstacle that breaks spatial symmetry will result in some modal conversion and scattering. For instance, guided modes can still be backscattered at the terminations of the waveguide, as usual. Implementations of

valley Hall crystals have been demonstrated for acoustic waves,^{4,53–55} elastic waves,^{56–59} but also water waves.^{60,61}

B. Quantum spin Hall crystals

In the description of the quantum spin Hall effect (QSHE) of graphene or semiconductor heterostructures, the bandgap at a Dirac point can be opened by strong spin-orbit coupling.⁴⁷ The system can be described as two copies of a quantum Hall system for which electrons with spin up or down feel opposite magnetic fields; as a whole, time-reversal is not broken. At time-reversal-invariant points, electronic states are twofold degenerate and form Kramers pairs (one spin-up state and one spin-down state). At an edge, there appear two oppositely propagating and dispersive edge states carrying opposite spins.

How can a classical wave system mimic the quantum spin Hall effect? We first need an equivalent of the Kramers pair for “quasi-particles” with no intrinsic spin. This can be implemented in a crystal lattice by a band folding technique.⁵² We can further understand how that happens by considering a hexagonal unit-cell for the honeycomb crystal, as depicted in Fig. 6(a). The hexagonal unit-cell is not primitive, since its area is three times larger than the original

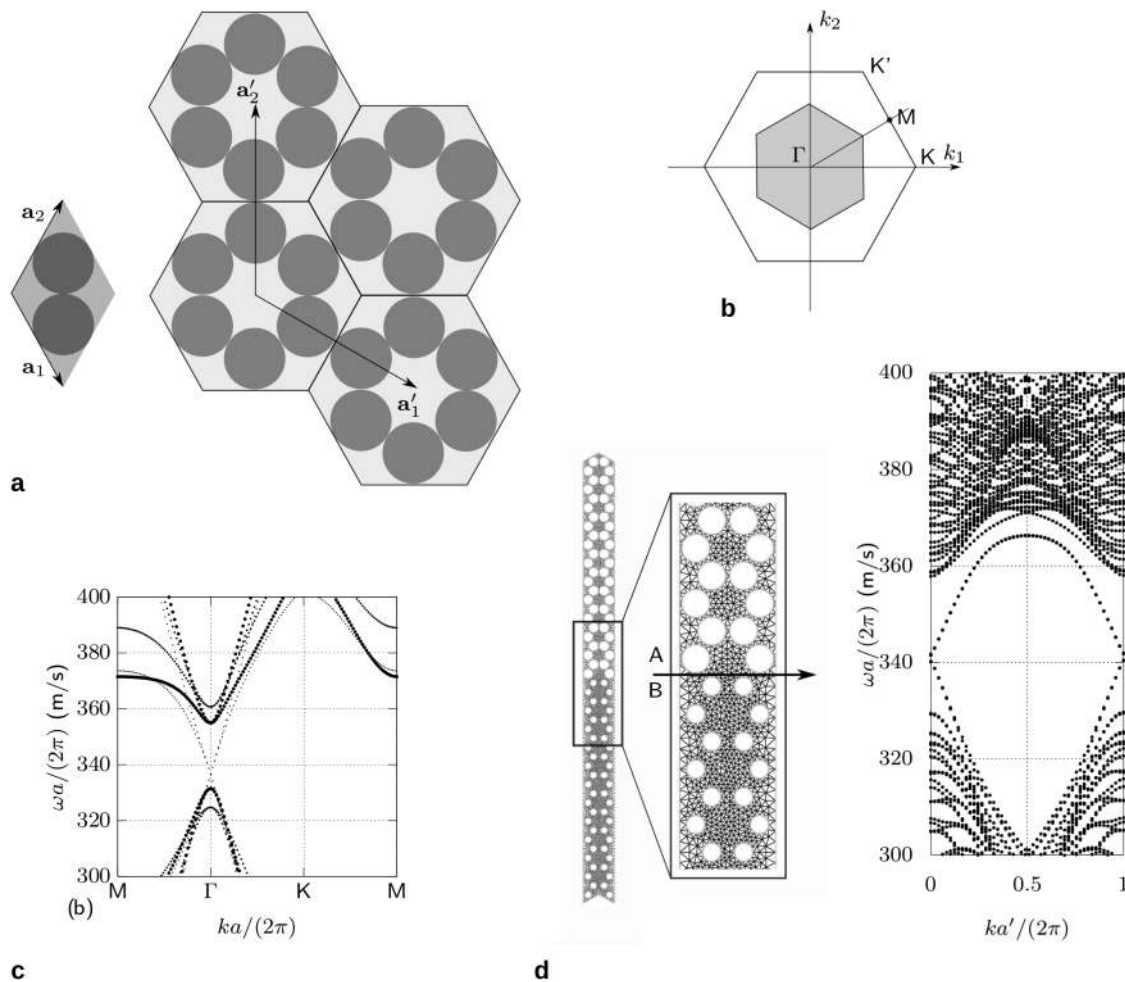


FIG. 6. Quantum spin Hall crystals. (a) The rhombohedral primitive unit-cell of the honeycomb crystal and its non-primitive hexagonal-unit cell are shown. (b) The first Brillouin zone shrinks when passing from the primitive to the hexagonal unit-cell. (c) A double Dirac cone is formed by degeneracy for an accidental value of d/a . Continuously tuning that parameter yields a topological transition that breaks the double Dirac cone and opens a complete bandgap. (d) A domain wall between crystals A ($d/a = 0.5196$) and B ($d/a = 0.3464$) supports a pair of non-interacting guided waves.

primitive unit-cell. The first Brillouin zone in Fig. 6(b) is a hexagon rotated by $\pi/6$ compared to the initial first Brillouin zone and has a surface reduced by one third. High-symmetry points K and K' of the initial Brillouin zone are now reciprocal lattice translations of point Γ in the transformed Brillouin zones. Hence, band folding results from crystal symmetry and interference of the folded bands opens the gap at the Γ point.

The band folding trick is still not sufficient, since a topological transition is needed. The second step is then to rely on an accidental degeneracy at the Γ point of the two groups of folded bands. For the sonic crystal of rigid cylinders in air, such an accidental fourfold degeneracy occurs for $d/a = 0.4536$,⁶³ as shown in Fig. 6(c). If d/a is increased or decreased continuously around the transition value, then the bandgap opens at the Γ point, a signature of a topological transition. It should be noted that varying d/a is not the only

option to achieve the topological transition, since any real parameter that preserves the space group of the crystal can be selected. For instance, one can move the inclusions toward or away from the unit-cell center.⁶²

Waves guided along a domain can be obtained similarly to the valley Hall case by exploiting the topological transition. We consider in Fig. 6(d) a domain wall between crystals A ($d/a = 0.5196$) and B ($d/a = 0.3464$). The domain wall is along the transformed ΓK direction or equivalently the original ΓM direction of the honeycomb crystal. The lattice constant of the supercell is $a' = \sqrt{3}a$. Two guided bands are found, as expected from our initial discussion, and each can be associated with a Kramers-like pair of states. Dispersion is almost linear close to the Γ point. The common bandgap of crystals A and B is not very large, and the exponential decay away from the domain wall is slow; hence, many rows are required for the supercell

to operate correctly. Besides the acoustic case,⁶³ quantum spin Hall phononic crystals for elastic waves have been proposed.^{64,65}

VI. CONCLUSION

In this Research Update, we have summarized the principles and the properties of phononic crystal waveguides. The basic idea is to replace the cladding of homogeneous waveguides with a crystal with a wide complete bandgap. Guidance can then be obtained inside a homogeneous core, a sequence of coupled defects, or at an interface or domain wall by relying on a topological transition. Those possible choices result in different dispersion properties. Linear defect and coupled-resonator phononic waveguides are now often considered in the context of tunable manipulation of acoustic or elastic waves.⁶⁶ The goal is then to design metamaterial structures for active or smart wave control. Topological⁴⁶ phononic crystal waveguides are presently attracting a lot of attention because they can provide waveguides with backscattering immunity, for instance, protected by symmetry. More progress is required to increase their bandwidth of operation, which is presently limited by the necessary topological transition around an initially closed gap.

ACKNOWLEDGMENTS

The author acknowledges support by the EIPHI Graduate School (Contract No. ANR-17-EURE-0002).

DATA AVAILABILITY

The data that support the findings of this study are available from the corresponding author upon reasonable request.

REFERENCES

- M. S. Kushwaha, P. Halevi, L. Dobrzynski, and B. Djafari-Rouhani, "Acoustic band structure of periodic elastic composites," *Phys. Rev. Lett.* **71**, 2022–2025 (1993).
- Y. Pennec, J. O. Vasseur, B. Djafari-Rouhani, L. Dobrzynski, and P. A. Deymier, "Two-dimensional phononic crystals: Examples and applications," *Surf. Sci. Rep.* **65**, 229–291 (2010).
- V. Laude, *Phononic Crystals: Artificial Crystals for Sonic, Acoustic, and Elastic Waves*, 2nd ed. (De Gruyter, Berlin, 2020).
- J. Lu, C. Qiu, L. Ye, X. Fan, M. Ke, F. Zhang, and Z. Liu, "Observation of topological valley transport of sound in sonic crystals," *Nat. Phys.* **13**, 369–374 (2017).
- S. Mohammadi, A. A. Eftekhar, W. D. Hunt, and A. Adibi, "High-Q micromechanical resonators in a two-dimensional phononic crystal slab," *Appl. Phys. Lett.* **94**, 051906 (2009).
- P. H. Otsuka, K. Nanri, O. Matsuda, M. Tomoda, D. M. Profunser, I. A. Veres, S. Danworaphong, A. Khelif, S. Benchabane, V. Laude, and O. B. Wright, "Broadband evolution of phononic-crystal-waveguide eigenstates in real- and k-spaces," *Sci. Rep.* **3**, 3351 (2013).
- S. Benchabane, O. Gaiffe, R. Salut, G. Ulliach, V. Laude, and K. Kokkonen, "Guidance of surface waves in a micron-scale phononic crystal line-defect waveguide," *Appl. Phys. Lett.* **106**, 081903 (2015).
- A. H. Safavi-Naeini and O. Painter, "Design of optomechanical cavities and waveguides on a simultaneous bandgap phononic-photon crystal slab," *Opt. Express* **18**, 14926–14943 (2010).
- A. H. Safavi-Naeini, J. T. Hill, S. Meenehan, J. Chan, S. Gröblacher, and O. Painter, "Two-dimensional phononic-photon band gap optomechanical crystal cavity," *Phys. Rev. Lett.* **112**, 153603 (2014).
- C. Brendel, V. Peano, O. Painter, and F. Marquardt, "Snowflake phononic topological insulator at the nanoscale," *Phys. Rev. B* **97**, 020102 (2018).
- Y.-F. Wang, Y.-S. Wang, and X.-X. Su, "Large bandgaps of two-dimensional phononic crystals with cross-like holes," *J. Appl. Phys.* **110**, 113520 (2011).
- F.-L. Hsiao, A. Khelif, H. Moubchir, A. Choujaa, C. C. Chen, and V. Laude, "Waveguiding inside the complete band gap of a phononic crystal slab," *Phys. Rev. E* **76**, 056601 (2007).
- M. F. Su, R. H. Olsson III, Z. C. Leseman, and I. El-Kady, "Realization of a phononic crystal operating at gigahertz frequencies," *Appl. Phys. Lett.* **96**, 053111 (2010).
- A. A. Maznev and V. E. Gusev, "Waveguiding by a locally resonant metasurface," *Phys. Rev. B* **92**, 115422 (2015).
- M. Ghasemi Baboly, C. M. Reinke, B. A. Griffin, I. El-Kady, and Z. C. Leseman, "Acoustic waveguiding in a silicon carbide phononic crystals at microwave frequencies," *Appl. Phys. Lett.* **112**, 103504 (2018).
- Y. Achaoui, A. Khelif, S. Benchabane, L. Robert, and V. Laude, "Experimental observation of locally-resonant and Bragg band gaps for surface guided waves in a phononic crystal of pillars," *Phys. Rev. B* **83**, 104201 (2011).
- Y. Achaoui, V. Laude, S. Benchabane, and A. Khelif, "Local resonances in phononic crystals and in random arrangements of pillars on a surface," *J. Appl. Phys.* **114**, 104503 (2013).
- Y. Pennec, B. Djafari Rouhani, H. Larabi, A. Akjouj, J. N. Gillet, J. O. Vasseur, and G. Thabet, "Phonon transport and waveguiding in a phononic crystal made up of cylindrical dots on a thin homogeneous plate," *Phys. Rev. B* **80**, 144302 (2009).
- R. Pourabolghasem, R. Dehghanasiri, A. A. Eftekhar, and A. Adibi, "Waveguiding effect in the gigahertz frequency range in pillar-based phononic-crystal slabs," *Phys. Rev. Appl.* **9**, 014013 (2018).
- M. Kurosu, D. Hatanaka, K. Onomitsu, and H. Yamaguchi, "On-chip temporal focusing of elastic waves in a phononic crystal waveguide," *Nat. Commun.* **9**, 1331 (2018).
- M. Oudich, M. B. Assouar, and Z. Hou, "Propagation of acoustic waves and waveguiding in a two-dimensional locally resonant phononic crystal plate," *Appl. Phys. Lett.* **97**, 193503 (2010).
- M. Addouche, M. A. Al-Lethawe, A. Elayouch, and A. Khelif, "Subwavelength waveguiding of surface phonons in pillars-based phononic crystal," *AIP Adv.* **4**, 124303 (2014).
- T. Miyashita and C. Inoue, "Numerical investigations of transmission and waveguide properties of sonic crystals by finite-difference time-domain method," *Jpn. J. Appl. Phys., Part 1* **40**, 3488 (2001).
- J. O. Vasseur, P. A. Deymier, B. Djafari-Rouhani, Y. Pennec, and A. C. Hladky-Hennion, "Absolute forbidden bands and waveguiding in two-dimensional phononic crystal plates," *Phys. Rev. B* **77**, 085415 (2008).
- Y. Achaoui, A. Khelif, S. Benchabane, and V. Laude, "Polarization state and level repulsion in two-dimensional phononic crystals and waveguides in the presence of material anisotropy," *J. Phys. D: Appl. Phys.* **43**, 185401 (2010).
- A. Khelif, B. Djafari-Rouhani, J. O. Vasseur, P. A. Deymier, P. Lambin, and L. Dobrzynski, "Transmittivity through straight and stublike waveguides in a two-dimensional phononic crystal," *Phys. Rev. B* **65**, 174308 (2002).
- A. Khelif, B. Djafari-Rouhani, J.-O. Vasseur, and P. A. Deymier, "Transmission and dispersion relations of perfect and defect-containing waveguide structures in phononic band gap material," *Phys. Rev. B* **68**, 024302 (2003).
- A. Khelif, A. Choujaa, B. Djafari-Rouhani, M. Wilm, S. Ballandras, and V. Laude, "Trapping and guiding of acoustic waves by defect modes in a full-band-gap ultrasonic crystal," *Phys. Rev. B* **68**, 214301 (2003).
- S. Benchabane, A. Khelif, A. Choujaa, B. Djafari-Rouhani, and V. Laude, "Interaction of waveguide and localized modes in a phononic crystal," *Europhys. Lett.* **71**, 570–575 (2005).
- V. Laude, J.-C. Beugnot, S. Benchabane, Y. Pennec, B. Djafari-Rouhani, N. Papanikolaou, J. M. Escalante, and A. Martinez, "Simultaneous guidance of slow photons and slow acoustic phonons in silicon phononic crystal slabs," *Opt. Express* **19**, 9690–9698 (2011).
- A. Khelif, A. Choujaa, S. Benchabane, B. Djafari-Rouhani, and V. Laude, "Guiding and bending of acoustic waves in highly confined phononic crystal waveguides," *Appl. Phys. Lett.* **84**, 4400 (2004).

- ³²Y.-F. Wang, T.-T. Wang, J.-W. Liang, Y.-S. Wang, and V. Laude, "Channeled spectrum in the transmission of phononic crystal waveguides," *J. Sound Vib.* **437**, 410–421 (2018).
- ³³S. Benchabane, A. Khelif, J.-Y. Rauch, L. Robert, and V. Laude, "Evidence for complete surface wave band gaps in a piezoelectric phononic crystal," *Phys. Rev. E* **73**, 065601(R) (2006).
- ³⁴R. H. Olsson III and I. El-Kady, "Microfabricated phononic crystal devices and applications," *Meas. Sci. Technol.* **20**, 012002 (2008).
- ³⁵D. Yudistira, Y. Pennec, B. Djafari Rouhani, S. Dupont, and V. Laude, "Non-radiative complete surface acoustic wave bandgap for finite-depth holey phononic crystal in lithium niobate," *Appl. Phys. Lett.* **100**, 061912 (2012).
- ³⁶V. Laude and M. E. Korotyaeva, "Stochastic excitation method for calculating the resolvent band structure of periodic media and waveguides," *Phys. Rev. B* **97**, 224110 (2018).
- ³⁷A. Yariv, Y. Xu, R. K. Lee, and A. Scherer, "Coupled-resonator optical waveguide: A proposal and analysis," *Opt. Lett.* **24**, 711 (1999).
- ³⁸S. Olivier, C. Smith, M. Rattier, H. Benisty, C. Weisbuch, T. Krauss, R. Houdré, and U. Oesterlé, "Miniband transmission in a photonic crystal coupled-resonator optical waveguide," *Opt. Lett.* **26**, 1019 (2001).
- ³⁹R. Sainidou, N. Stefanou, and A. Modinos, "Linear chain of weakly coupled defects in a three-dimensional phononic crystal: A model acoustic waveguide," *Phys. Rev. B* **74**, 172302 (2006).
- ⁴⁰J. M. Escalante, A. Martínez, and V. Laude, "Dispersion relation of coupled-resonator acoustic waveguides formed by defect cavities in a phononic crystal," *J. Phys. D: Appl. Phys.* **46**, 475301 (2013).
- ⁴¹J. Grgić, E. Campaioli, S. Raza, P. Bassi, and N. Mortensen, "Coupled-resonator optical waveguides: Q-factor and disorder influence," *Opt. Quantum Electron.* **42**, 511–519 (2011).
- ⁴²Y. Jin, Y. Pennec, Y. Pan, and B. Djafari-Rouhani, "Phononic crystal plate with hollow pillars actively controlled by fluid filling," *Crystals* **6**, 64 (2016).
- ⁴³Y.-F. Wang, T.-T. Wang, Y.-S. Wang, and V. Laude, "Reconfigurable phononic-crystal circuits formed by coupled acoustoelastic resonators," *Phys. Rev. Appl.* **8**, 014006 (2017).
- ⁴⁴T.-T. Wang, S. Bargiel, F. Lardet-Vieudrin, Y.-F. Wang, Y.-S. Wang, and V. Laude, "Collective resonances of a chain of coupled phononic microresonators," *Phys. Rev. Appl.* **13**, 014022 (2020).
- ⁴⁵J. Lu, C. Qiu, S. Xu, Y. Ye, M. Ke, and Z. Liu, "Dirac cones in two-dimensional artificial crystals for classical waves," *Phys. Rev. B* **89**, 134302 (2014).
- ⁴⁶G. Ma, M. Xiao, and C. T. Chan, "Topological phases in acoustic and mechanical systems," *Nat. Rev. Phys.* **1**, 281–294 (2019).
- ⁴⁷M. Z. Hasan and C. L. Kane, "Colloquium: Topological insulators," *Rev. Mod. Phys.* **82**, 3045–3067 (2010).
- ⁴⁸P. Delplace, D. Ullmo, and G. Montambaux, "Zak phase and the existence of edge states in graphene," *Phys. Rev. B* **84**, 195452 (2011).
- ⁴⁹R. Fleury, D. L. Sounas, C. F. Sieck, M. R. Haberman, and A. Alu, "Sound isolation and giant linear nonreciprocity in a compact acoustic circulator," *Science* **343**, 516–519 (2014).
- ⁵⁰Z. Yang, F. Gao, X. Shi, X. Lin, Z. Gao, Y. Chong, and B. Zhang, "Topological acoustics," *Phys. Rev. Lett.* **114**, 114301 (2015).
- ⁵¹A. B. Khanikaev, R. Fleury, S. H. Mousavi, and A. Alu, "Topologically robust sound propagation in an angular-momentum-biased graphene-like resonator lattice," *Nat. Commun.* **6**, 8260 (2015).
- ⁵²J. Lu, C. Qiu, M. Ke, and Z. Liu, "Valley vortex states in sonic crystals," *Phys. Rev. Lett.* **116**, 093901 (2016).
- ⁵³L. Ye, C. Qiu, J. Lu, X. Wen, Y. Shen, M. Ke, F. Zhang, and Z. Liu, "Observation of acoustic valley vortex states and valley-chirality locked beam splitting," *Phys. Rev. B* **95**, 174106 (2017).
- ⁵⁴Y. Shen, C. Qiu, X. Cai, L. Ye, J. Lu, M. Ke, and Z. Liu, "Valley-projected edge modes observed in underwater sonic crystals," *Appl. Phys. Lett.* **114**, 023501 (2019).
- ⁵⁵N. Laforge, R. Wiltshaw, R. V. Craster, V. Laude, J. A. Iglesias Martínez, G. Dupont, S. Guenneau, M. Kadic, and M. P. Makwana, "Acoustic topological circuitry in square and rectangular phononic crystals," *Phys. Rev. Appl.* **15**, 054056 (2021).
- ⁵⁶R. K. Pal and M. Ruzzene, "Edge waves in plates with resonators: An elastic analogue of the quantum valley Hall effect," *New J. Phys.* **19**, 025001 (2017).
- ⁵⁷J. Vila, R. K. Pal, and M. Ruzzene, "Observation of topological valley modes in an elastic hexagonal lattice," *Phys. Rev. B* **96**, 134307 (2017).
- ⁵⁸M. Yan, J. Lu, F. Li, W. Deng, X. Huang, J. Ma, and Z. Liu, "On-chip valley topological materials for elastic wave manipulation," *Nat. Mater.* **17**, 993–998 (2018).
- ⁵⁹H. Zhu, T.-W. Liu, and F. Semperlotti, "Design and experimental observation of valley-Hall edge states in diatomic-graphene-like elastic waveguides," *Phys. Rev. B* **97**, 174301 (2018).
- ⁶⁰N. Laforge, V. Laude, F. Chollet, A. Khelif, M. Kadic, Y. Guo, and R. Fleury, "Observation of topological gravity-capillary waves in a water wave crystal," *New J. Phys.* **21**, 083031 (2019).
- ⁶¹M. P. Makwana, N. Laforge, R. V. Craster, G. Dupont, S. Guenneau, V. Laude, and M. Kadic, "Experimental observations of topologically guided water waves within non-hexagonal structures," *Appl. Phys. Lett.* **116**, 131603 (2020).
- ⁶²L.-H. Wu and X. Hu, "Scheme for achieving a topological photonic crystal by using dielectric material," *Phys. Rev. Lett.* **114**, 223901 (2015).
- ⁶³C. He, X. Ni, H. Ge, X.-C. Sun, Y.-B. Chen, M.-H. Lu, X.-P. Liu, and Y.-F. Chen, "Acoustic topological insulator and robust one-way sound transport," *Nat. Phys.* **12**, 1124–1129 (2016).
- ⁶⁴B.-Z. Xia, T.-T. Liu, G.-L. Huang, H.-Q. Dai, J.-R. Jiao, X.-G. Zang, D.-J. Yu, S.-J. Zheng, and J. Liu, "Topological phononic insulator with robust pseudospin-dependent transport," *Phys. Rev. B* **96**, 094106 (2017).
- ⁶⁵M. Miniaci, R. Pal, B. Morvan, and M. Ruzzene, "Experimental observation of topologically protected helical edge modes in patterned elastic plates," *Phys. Rev. X* **8**, 031074 (2018).
- ⁶⁶Y.-F. Wang, Y.-Z. Wang, B. Wu, W. Chen, and Y.-S. Wang, "Tunable and active phononic crystals and metamaterials," *Appl. Mech. Rev.* **72**, 040801 (2020).